Atmospheric water vapor transport associated with typical anomalous summer rainfall patterns in China

Tian-Jun Zhou and Ru-Cong Yu

State Key Laboratory of Numerical Modeling for Atmospheric Sciences and Geophysical Fluid Dynamics, Institute of Atmospheric Physics, Chinese Academy of Sciences, Beijing, China

Received 2 September 2004; revised 19 January 2005; accepted 9 February 2005; published 20 April 2005.

[1] This paper attempts to reveal the atmospheric water vapor transports associated with typical anomalous summer rainfall patterns in China. The results show that origins of water vapor supply related to anomalous rainfall patterns are different from those related to the normal monsoon rainfall. Anomalous pattern 1, with a heavier rainbelt along the middle and lower reaches of the Yangtze River valley, follows from a convergence of the tropical southwest water vapor transport with the midlatitude northeast water vapor transport; the tropical water vapor transport comes directly from the Bay of Bengal and the South China Sea but originally from the Philippine Sea. The anomalous water vapor transport is associated with a southwestward extension of the western Pacific subtropical high and a southward shift of the upper East Asian jet stream. Anomalous pattern 2, with a main rainbelt along the Huaihe River valley, is supported by the convergence of the subtropical southwest water vapor with the midlatitude water vapor transport. The subtropical branch comes directly from the South China Sea but originally from the East China Sea and the adjacent subtropical Pacific to the further east along 20–25°N. The background large-scale circulation change includes a northwestward extension of the western Pacific subtropical high and an eastward shift of the upper jet stream. Although the cross-equator flows including the Somali jet supply abundant water vapor for the normal condition of June, July, and August rainfall over China, the tropical water vapor transports related to typical anomalous rainfall anomalies originate from the tropical western Pacific Ocean. The northward transport of anomalous warm water vapor occurs mainly in the lower troposphere, while the transport of midlatitude cold water vapor occurs briefly in the upper troposphere.

Citation: Zhou, T.-J., and R.-C. Yu (2005), Atmospheric water vapor transport associated with typical anomalous summer rainfall patterns in China, *J. Geophys. Res.*, *110*, D08104, doi:10.1029/2004JD005413.

1. Introduction

[2] East China experiences a typical monsoon climate. During the summer, the bulk of central and eastern Asia is under the influence of southwest surface winds accompanied by heavy rain, and a generally hot and humid climate. A strong summer monsoon is accompanied with more rainfall in North China, while a weak summer monsoon is usually followed by heavier rainfall along the Yangtze River valley. Monsoon related droughts and floods have had enormous social and economic impacts on China and the countries of Southeast Asia, which form a large segment of the world's population [*Lau and Li*, 1984; *Tao and Chen*, 1987; *Ding*, 1994]. As a result, understanding the mechanisms and physical processes governing the monsoon variability has been an issue of considerable urgency, and much effort has been devoted to the problem in the past decades [e.g., *Webster and Yang*, 1992; *Li and Yanai*, 1996; *Hu*, 1997; *Meehl and Arblaster*, 1998; *B. Wang et al.*, 2000; *W. C. Wang et al.*, 2000; *Zhou and Li*, 2002; *Gong and Ho*, 2003].

[3] The hydrological process plays an important role in determining the scale of the major atmospheric circulation patterns [*Webster*, 1994]. Anomalous rainfall is directly related to the moisture supply. The water vapor transport is one of the most important components of the East Asian monsoon system. A large amount of water vapor is carried from the adjacent oceans to the East Asian monsoon region by the large-scale monsoon circulations. Progress in the understanding of water vapor transport will greatly advance our knowledge of the anomalous monsoon rainfall. Research from Chinese scientists on atmospheric water vapor over East Asia dates back to the 1950s, but it is limited by a dearth of accurate data [*Xu*, 1958; *Xie and Dai*, 1959]. This situation has changed in recent years. Analysis of Chinese radiosonde data from 1970 to 1990 shows that an increase (decrease) in precipitable water over China is associated with an increase (decrease) of precipitation in

0148-0227/05/2004JD005413$09.00

most parts of China. Interannual variations of precipitable water and precipitation are significantly correlated [*Zhai and Eskridge*, 1997]. Although strong convergence of water vapor associated with the monsoon circulation dominates both southern and eastern Asia in boreal summer [*Rasmusson and Mo*, 1996; *Zhou et al.*, 1999], there exist remarkable difference between the water vapor transport over the East Asian monsoon region and that over the Indian monsoon region. The water vapor convergence over East Asia is mainly due to the water vapor advection caused by the monsoon flow, while the wind convergence plays an important role in the water vapor convergence over the Indian monsoon region [*Huang et al.*, 1998]. The East Asian summer monsoon is affected not only by the Indian summer monsoon flow, but also by the western Pacific subtropical high and the midlatitude circulations [*Lau and Li*, 1984; *Tao and Chen*, 1987; *Ding*, 1994]. Traditionally, the Somali jet, the cross-equator flow associated with the Australian cold high, and the east flow from the south of the western Pacific subtropical high are regarded as the key moisture transport passes for heavy rainfall over eastern China [*Tao and Chen*, 1987]. Later cases studies, however, emphasize the contribution of the moisture transport from the Bay of Bengal, the South China Sea and the western Pacific Ocean [*Ninomiya and Kobayashi*, 1999; *Ninomiya*, 1999; *Ding and Sun*, 2001; *Ding and Hu*, 2003]. Estimations using ECMWF-WMO twice-daily global analysis data for the period 1980–1996 show that the Indian monsoon circulation plays a small part in determining the character of the differences between the wet and dry years of southeastern China (25°–35°N, 110°–120°E), and the water vapor that supports the summer rainfall over this area comes mainly from the South China Sea and the western Pacific Ocean [*Simmonds et al.*, 1999]. The water vapor transport from the Indian summer monsoon is in inverse proportion to that over East Asia: more Indian monsoon water vapor transport corresponds to less water vapor transport over East Asia and less rainfall in the middle and lower reaches of the Yangtze River valley [*Zhang*, 2001].

[4] The main objective of this paper is to reveal the water vapor transports anomalies associated with typical anomalous rainfall patterns. Forecasting monsoon variability, and particularly the associated rainfall anomalies, has been the focus of Chinese meteorologists. Although there exist strong year-to-year variations of the main summer rainbelts, operational short-term climate predictions performed by forecasters at the National Climate Center of the China Meteorological Administration categorize the anomalous summer monsoon rainbelts into three kinds of typical patterns with centers locating respectively in the middle and lower reaches of the Yangtze River valley, the Huaihe River valley, and the Yellow River valley [*Zhao*, 1999]. Former studies on water vapor transport over China have focused mainly on either the normal monsoon rainfall conditions or on specific cases. The transports associated with the typical anomalous rainfall patterns used in operational forecasts are not, however, well addressed. The analyses presented here show that although the tropical water vapor transports related to typical anomalous rainbelts come directly from either the South China Sea or the Bay of Bengal or both, their ultimate origins are from the tropical western Pacific. Different from the moisture source responsible for the normal conditions of summer rainfall, no contribution from the cross-equator transports such as the Somali jet is found for typical anomalous rainbelts.

[5] The outline of the paper is as follows: section 2 introduces the data and the methodology, and section 3 describes the background water vapor transport and the definitions of typical anomalous summer monsoon rainfall patterns in China. The water vapor transports associated with typical anomalous rainbelts are presented in section 4, including discussions on the large-scale circulation changes. Concluding remarks are given in section 5.

2. Data and Methodology

[6] Global reanalysis data sets provided by NCEP/NCAR for boreal summer (June, July, and August (JJA)) for the period 1951–1999 are used to estimate the terms of the atmospheric water vapor transport [*Kalnay et al.*, 1996]. An evaluation of the NCEP/NCAR reanalysis data moisture fields, the moisture transport, and divergence in the atmosphere has been carried out by *Trenberth and Guiliemot* [1995] and *Zhou et al.* [1999]. The physical variables used in this study include the monthly specific humidity, and the meridional and zonal wind components at eight standard pressure levels, namely, 1000, 925, 850, 700, 600, 500, 400, and 300 hPa. The geopotential height at 500 hPa and the zonal and meridional winds at 200 hPa are used to describe the circulation change. The surface pressure is used to treat the impact of topography. Another source of atmospheric data used for estimating the water vapor flux is from the ECMWF reanalyses (hereinafter referred to as ERA40; see http://www.ecmwf.int/research/era/), where the monthly meridional and zonal wind components, air temperature and relative humidity at two standard pressure levels (850 hPa and 500 hPa) are used. The relative humidity RH is transformed to specific humidity q by using the standard formula,

$$q = 0.622 \cdot \frac{e_s}{p - e_s} \cdot RH \tag{1}$$

where e_s is the saturation pressure of water vapor that can be calculated from the air temperature, and p is the atmospheric pressure. The ERA40 data used in the current analysis covers a shorter time period from 1958 to 1999.

[7] The data set of monthly stational precipitation (1951–1999) from China Meteorological Administration is used. This data set consists of the monthly averaged precipitation of 160 stations in China and has been widely used in the study of the East Asian monsoon climate [e.g., *Nitta and Hu*, 1996; *Hu*, 1997; *Simmonds et al.*, 1999; *Gong and Ho*, 2003; *Hu et al.*, 2003]. Figure 1a shows the distribution of the stations. Most of the stations are located in eastern China. This does not cause trouble to our research target, since the monsoon rainfall mainly dominates the southern and eastern part of Mainland China, where we have a better coverage of observational stations. As shown in Figure 1a, strong interannual variations of the summer precipitation exist mainly to the east of 100°E, where our target regions are located.

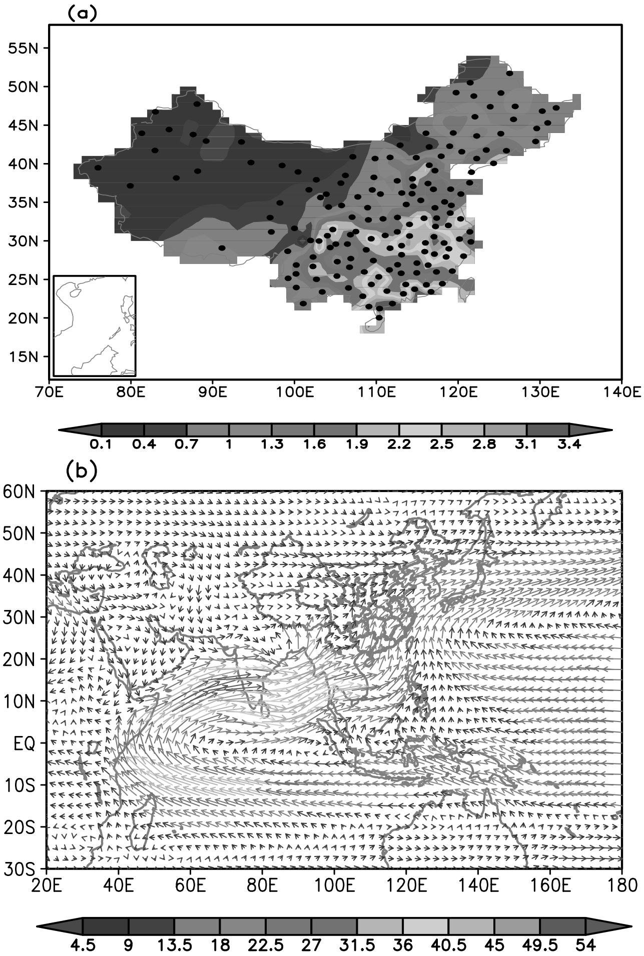

Figure 1. (a) Standard deviation of JJA mean rainfall revealed by the station data (mm/day). Dots indicate locations of the observational stations. (b) Vertically integrated climate mean (1951–1999 average) JJA water vapor transport (kg × m^{-1} s^{-1}). The coloring indicates the magnitude of the moisture flux vector. See color version of this figure at back of this issue.

[8] The vertically integrated moisture flux can be expressed as

$$\vec{Q} = \frac{1}{g}\int_0^{p_s} q\vec{V}dp \qquad (2)$$

where q is specific humidity, $\vec{v}$ is the horizontal wind vector, p is the pressure, p_s is the surface pressure, and g is the acceleration due to gravity. Since the NCEP/NCAR reanalysis sets the specific humidity to zero above 300 hPa, the vertical integration of equation (2) is performed from the surface to 300 hPa. The missing data above 300 hPa has a nearly negligible impact on the result because of the concentration of water vapor in the lower troposphere. Previous estimation indicates that even at tropical oceans, the maximum value of the neglected water vapor above 300 hPa is limited to within 2–3 cm/year in terms of the freshwater flux [*Zhou*, 2003].

[9] The water vapor transport can be separated into two parts: the stationary and the transient components. The former is calculated by using monthly mean data, while the latter is evaluated as departures from individual monthly mean values by using four-times daily averaged data. Previous analyses indicate that the stationary component dominates the total transport of the water vapor and its interannual variation over East Asia, while the transient eddies play negligible roles [*Zhou et al.*, 1999; *Simmonds et al.*, 1999]. The analyses to be performed in this study will accordingly focus mainly on the dominant stationary component.

3. Background Water Vapor Transport and Typical Anomalous Summer Rainfall Patterns in China

[10] The background climate mean water vapor transport closely resembles the large-scale monsoon circulation in the lower troposphere [e.g., *Zhou and Li*, 2002]. Figure 1b shows the boreal summer (JJA mean) total water vapor transport. East Asia mainly has three branches of tropical water vapor transport for normal climatological conditions: The first is the strong transport by the Indian (or southwest) monsoon, which is linked to the robust cross-equator Somali jet and brings abundant moisture from the Arabian Sea and the Bay of Bengal, crossing the Indochina Peninsula and the South China Sea into eastern China; The second is the transport by the Southeast Asian monsoon, which comes from the western Pacific and brings moisture from the tropical Pacific Ocean into eastern China; The third is the cross-equator flow straddling 105°E–150°E, which is the weakest one among these three branches. In addition, North China is affected by a weak water vapor transport of the midlatitude westerlies. These main branches of water

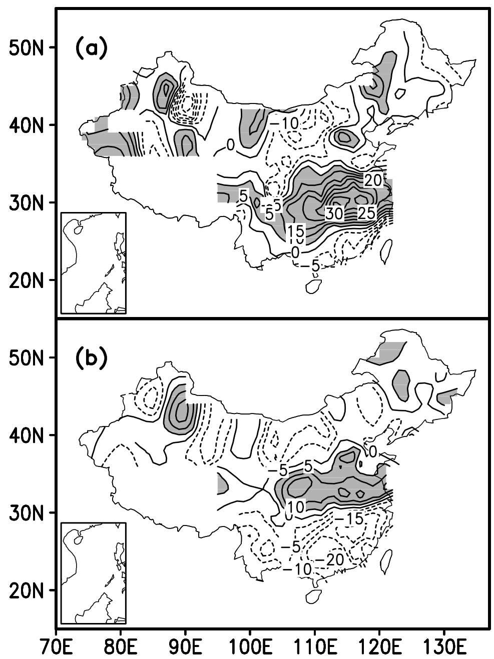

Figure 2. The leading modes of JJA mean rainfall for 1951–1999. (a) EOF1 and (b) EOF2. Patterns are shown as percentage of rainfall anomaly relative to climate mean state associated with one standard deviation of the corresponding PC change.

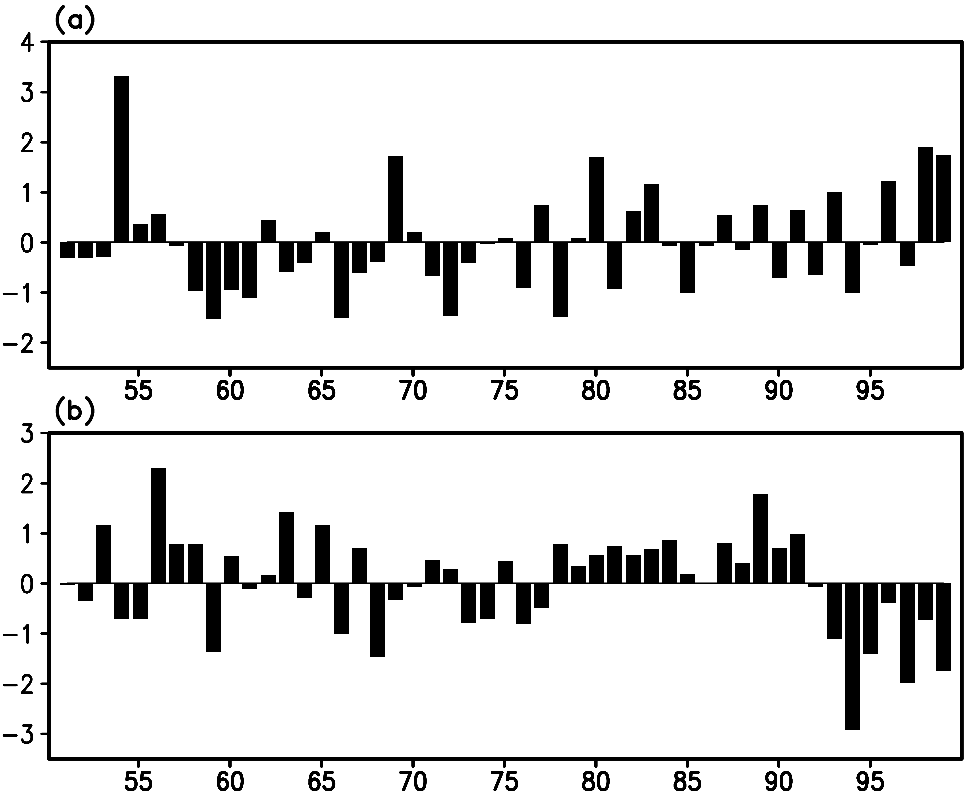

Figure 3. The normalized principal component corresponding to the leading mode of (a) EOF1 and (b) EOF2.

vapor pathways bear great similarities to previous analyses based on different data sets or time periods [*Tao and Chen*, 1987; *Huang et al.*, 1998; *Simmonds et al.*, 1999; *Zhang*, 2001]. Note that this is the case for normal monsoon rainfall, but what we care about and will address here are the water vapor transports anomalies accompanying typical anomalous rainfall patterns.

[11] To reveal the spatial patterns of summertime monsoon rainfall variation, empirical orthogonal function (EOF) analysis is applied to the observed JJA mean precipitation anomalies. The first two leading modes are shown in Figure 2. These two modes account for 16.3% and 12.4% of the total variance, respectively. They are well separated from each other according to the criterion of *North et al.* [1982]. The corresponding normalized principal components (PCs) are given in Figure 3. These two leading EOF modes essentially correspond to the typical anomalous summer monsoon rainfall patterns defined by the National Climate Center of the China Meteorological Administration in operational short-term climate predictions according to the historical statistics. They are usually called the southern pattern in response to Figure 2a, and the middle pattern in response to Figure 2b [*Zhao*, 1999].

[12] In the first leading mode, namely, the southern pattern (Figure 2a), positive anomalies dominate the middle and lower reaches of the Yangtze River valley. Associated with one standard deviation change of the corresponding PC, the summer precipitation increases by at most 30%. Combing Figure 3a with Figure 2a, we can observe that for some typical years such as 1954 and 1998, the central precipitation increased nearly 100% and 60% respectively relative to the climate mean conditions.

[13] In the second EOF mode, namely, the middle pattern (Figure 2b), a heavier rainbelt controls the area between the Yangtze River valley and the Yellow River valley, with centers along the Huaihe River valley (approximately 5 degrees north of the Yangtze River valley). For some typical years such as 1956 and 1989, the central precipitation increased approximately 35% and 30% respectively relative to the normal conditions. This anomaly is slightly weaker than that of EOF1.

[14] In addition, the third EOF mode of summer rainfall appears as heavier precipitation over north China including the lower reaches of the Yellow River valley, together with a secondary stronger rainfall center locating in southwest China (figure omitted). This mode explains 6.7% of the total variance and corresponds to the northern pattern defined in operational prediction [*Zhao*, 1999]. Further analysis reveals, however, that it is not well separated from the fourth EOF mode according to North's criterion [*North et al.*, 1982]. So in the following analysis, we will emphasize the first two leading modes.

[15] These two typical patterns (EOF1 and EOF2) of anomalous summer rainfall will be referred to as patterns 1 and 2, respectively, in the following discussions. The main features of these two typical anomalous rainbelts are encapsulated in Table 1.

4. Anomalous Water Vapor Transport

4.1. Vertically Integrated Transport

[16] The water vapor transport anomalies associated with typical anomalous rainfall patterns can be estimated by regressing the vertically integrated moisture flux anomalies

Table 1. Typical Anomalous June, July, and August Rainfall Patterns in East China and the Associated Water Vapor Transport

Typical Anomalous Rainfall Patterns	Pattern 1	Pattern 2
Main rain belts	along the middle and lower reaches of the Yangtze River valley	along the Huaihe River valley
Water vapor transport	convergence of tropical southwest water vapor with midlatitude northeast water vapor. Tropical water vapor comes directly from the Bay of Bengal and the South China Sea but the origin can be traced back to the Philippine Sea	convergence of the subtropical southwest water vapor with the midlatitude water vapor; the subtropical branch comes directly from the South China Sea but originally from the East China Sea and the adjacent subtropical Pacific to the further east along 20–25°N
Large-scale circulation	southwestward extension of the western Pacific subtropical high and southward shift of the east Asian jet stream	northwestward extension of the western Pacific subtropical high and eastward shift of the upper jet stream

upon the corresponding PCs of rainfall EOF modes. The result for anomalous rainfall pattern 1 is shown in Figure 4a. Accompanying heavier rainfall along the middle and lower reaches of the Yangtze River valley, a strong convergence of the tropical and subtropical water vapor transport is found above the anomalous rainbelt. The warmer tropical water vapor flows northeastwardly along the coastline of the east Asian continent before meeting the cold subtropical water vapor coming from higher latitudes. The anomalous tropical water vapor transport has two branches, one from the South China Sea and the other from the Bay of Bengal. Both of them, however, ultimately originate from the Philippine Sea. No significant anomalous transport from the climatological position of the Somali jet can be found.

[17] The water vapor transport is closely linked to the atmospheric circulation change. Previous studies have found that the East Asia summer monsoon is greatly controlled by the western Pacific subtropical high in the lower atmosphere and the East Asia westerly jet stream in the higher atmosphere [e.g., *Tao and Chen*, 1987]. To show the circulation change dominating the water vapor transport, the gridded 500 hPa geopotential height anomalies (Z500) and 200 hPa zonal wind anomalies (U200) are respectively regressed upon the PC of the rainfall EOF1. The results are depicted in Figures 4b–4c. Relative to its normal climatic position, the western Pacific subtropical high extends southwestward. This anomalous circulation pattern benefits the northeastward transport of the warmer tropical water vapor from the Bay of Bengal and the South China Sea along the northwestern flank of the western Pacific subtropical high. At upper levels, the westerly jet stream moves southward. The intensified zonal wind crossing 120°E along 30°N indicates a stronger high-level zonal divergence there. This favors stronger convections, which are responsible for the heavier rainfall. It should be stressed that it is the convergence of the warmer tropical water vapor with the colder subtropical water vapor that results in the heavier rainfall along the middle and lower reaches of the Yangtze River valley. Former studies have emphasized mainly the tropical water vapor flow; but the contribution of the subtropical transport should not be ignored. Both the north flow from the midlatitudes and the east flow from the Pacific Ocean supply the subtropical water vapor transport.

[18] The water vapor transport anomalies associated with anomalous rainfall pattern 2 is shown in Figure 5a. The subtropical water vapor converges with the midlatitude water vapor above the main rainbelt between the lower reaches of the Yangtze River valley and the Yellow River valley. The anomalous northeastward subtropical water vapor along eastern China comes directly from the South China Sea but has a tropical West Pacific origin. Neither the water vapor from the Bay of Bengal nor the cross-equator water vapor transport from the Southern Hemisphere supplies the anomalous convergence over the Huaihe River valley. The origin of the anomalous water vapor transport is ultimately the East China Sea and the adjacent subtropical Pacific further east along 20–25°N. The northward shift and westward extension of the western Pacific subtropical high (Figure 5b), together with an eastward extension of the upper 200 hPa jet stream center and the associated stronger zonal divergence there (Figure 5c), favor the supply of warmer subtropical water vapor and its succedent convergence with the relatively colder midlatitude water vapor.

[19] Inspections of Figures 5b–5c reveal clear wave propagation patterns. There exist positive anomalies between 20°N and 35°N in Figure 5b. These positive anomalies extend from the east China continent eastward toward the Japan Islands. Negative anomalies are found both to the south and to the north of the positive anomaly regions. Similar wave-like anomalies propagate from the western tropical Pacific to East Siberia via the eastern coast of China in Figure 5c. This wave propagation pattern in East Asia from subtropics to extratropics corresponds quite well to the Pacific Japan (PJ) or the East Asia Pacific (EAP) teleconnection pattern, which is believed to be the result of Rossby wave dispersion due to anomalous heating around the Philippines [*Nitta*, 1987; *Huang and Sun*, 1992]. Further discussion on the mechanism dominating the PJ/EAP pattern is beyond the scope of the current research. What we want to stress here is that the PJ/EAP pattern is clear not only for the anomalous rainfall pattern 2 but also for anomalous rainfall pattern 1. The anomalous circulation in Figure 4c also has the wave-like feature, which is similar to that in Figure 5c but slightly different in magnitude and centers. The difference potentially reflects the different heating sources related to these two different precipitation

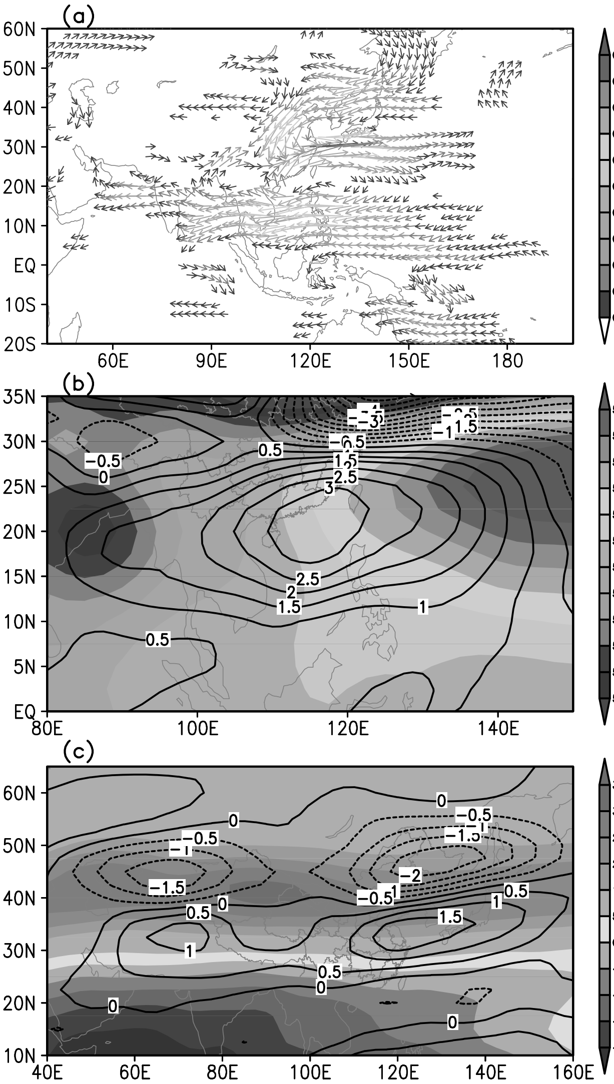

Figure 4. Anomalies of (a) vertically integrated water vapor transport in kg $\times$ m^{-1}s^{-1}, (b) 500−hPa geopotential height in meters, and (c) 200-hPa zonal wind in ms^{-1} regressed upon the PC of rainfall EOF1. The coloring in Figure 4a indicates the magnitude of the moisture flux vector. The climate mean conditions of Z500 and U200 are the colored backgrounds of Figures 4b and 4c, respectively. See color version of this figure at back of this issue.

patterns in China. Previous work found that both interannual and intraseasonal variabilities of the East Asian summer monsoon are greatly influenced by the convective activities in the warm pool. The monsoon rainfall is generally below normal in East Asia (briefly along the middle and lower reaches of the Yangtze River valley) and the abrupt change of the monsoon circulation is obvious in the summer of strong convective activities [*Huang and Sun*, 1992; *Ren and Huang*, 1999]. Hence the water vapor transport anomalies associated with two typical anomalous rainfall patterns in China can be potentially modulated by the PJ/EAP teleconnection patterns associated with the tropical heating.

[20] In addition, the time series of EOF1 clearly has a linear trend (Figure 3a), indicating a shift in the summer rainfall along the Yangtze River valley in the past decades. Variations of the sea surface temperatures of the tropical Indian Ocean are suggested to be responsible for this rainfall shift through the changes in the subtropical northwestern Pacific high [*Gong and Ho*, 2002; *Hu et al.*, 2003]. The emphasis here is the obvious decadal variation in the time series of EOF2 (Figure 3b), which is less noted in previous works. Combined with the corresponding anomalous rainfall patterns (Figure 2b), this indicates that the summer rainfall has been shifted from above normal to below normal in the Huaihe River valley since 1992. The opposite change occurred to the south. The flooding of south China in the 1990s was also noted by *Wang et al.* [2002], and the driving mechanism is partly attributed to the succession of El Nino events in the 1990s [*Xiao and Gong*, 2000]. From Figure 5a (except reversing the vector arrow directions in response to the negative trend in the 1990s), we can find that a wetter south China in the 1990s is supported by the convergence of two branches of water vapor transport: one from the tropical western Pacific (120°–140°E, 10°N) which passes through the South China Sea, and the other is from the extratropical high latitudes appearing as northeast flows. A large part of the northeast

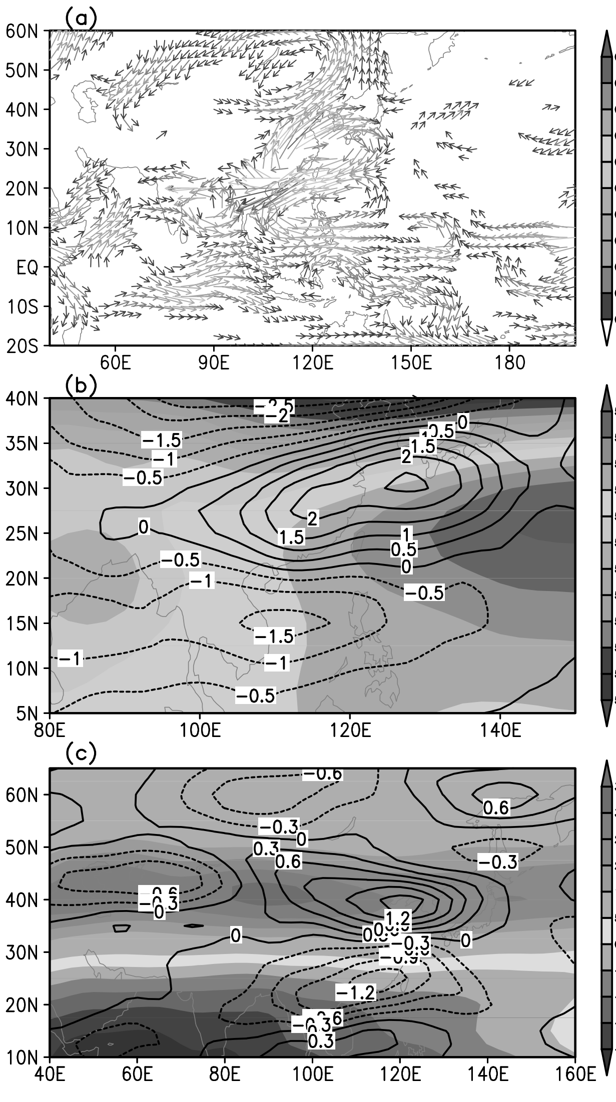

Figure 5. Same as Figure 4 except for EOF2. See color version of this figure at back of this issue.

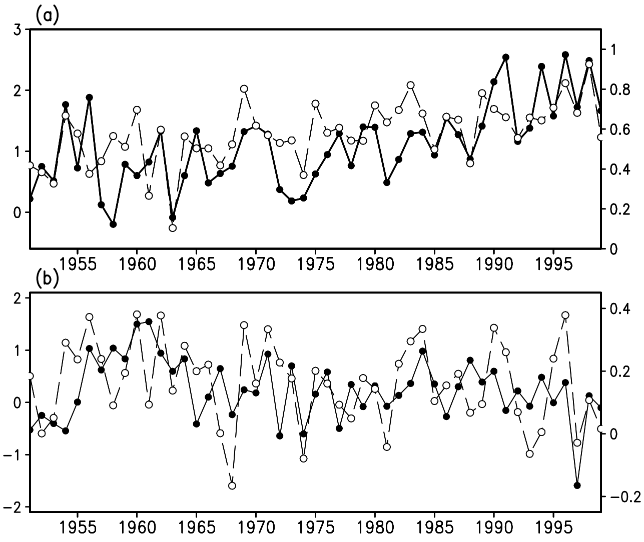

Figure 6. Time evolution of the water vapor convergence (solid line with solid circles in units of 10^{-6} kg $\times$ m^{-2} s^{-1} and corresponding to the right axis label) and 200-hPa wind vector divergence (dashed line with open circles in units of 10^{-6} s^{-1} and corresponding to the left axis label) averaged over (a) the lower reaches of the Yangtze River valley (112.5–122.5°E, 28–34°N) and (b) the Huaihe River valley (115–125°E, 32–36°N).

flows can be traced back to the East China Sea and the adjacent subtropical Pacific.

[21] Although for ease of comparison with the climate mean condition, no significant tests are shown in Figures 4–5, significant tests have been preformed on the regression equations by using a *F* test, and the results demonstrate that the main anomaly patterns over the target regions are significant at 95% confidence levels (figures omitted). The relationships between the moisture convergence, the circulation change and the typical anomalous rainfall patterns are further revealed in a concise way. The convergence of the water vapor transport and the divergence of 200 hPa wind vectors are averaged respectively over the main rainbelt area associated with typical anomalous rainfall patterns seen in Figure 2. The resulting time series are shown in Figure 6. The flooding years over the target regions generally follow from stronger water vapor convergence and more intense convection appearing as stronger divergence at 200 hPa. The linear trends in Figure 6a and 6b correspond well to the decadal-scale rainfall variations discussed above, supporting as the evidence from the large-scale circulation and water vapor supply background. For heavier rainfall over the middle and lower reaches of the Yangtze River valley, the PC1 has a correlation coefficient of 0.47 with the 200hPa divergence index and 0.50 with the water vapor convergence index. After removing the linear trends, the corresponding correlation coefficients decrease slightly to 0.45 and 0.50, respectively. For heavier rainfall over the Huaihe River basin, the corresponding correlation coefficients for PC2 are 0.34 and 0.31, respectively. After removing the linear trends, the correlation coefficients change to be 0.31 and 0.28 respectively. These correlation coefficients are statistically significant at the 95% confidence level, except that the value of 0.28 is significant at 90% confidence level. Compared with the statistics for PC1, the correlation coefficients for PC2 are relatively lower. The reason is that in contrast to EOF1 where positive anomalies over the target regions briefly dominate the general patterns, EOF2 reveals a pattern with heavier rainfall along the Huaihe River valley and less rainfall over south China, yet the southern negative anomaly is stronger than the positive anomaly in absolute intensity (Figures 2a–2b). In analyses on the time evolution of PC2, the moisture convergence index and the 200 hPa divergence index averaged over the south China negative anomaly region both get higher correlation coefficients. If we directly define the typical anomalous rainfall pattern index as the regionally averaged anomalous rainfall over the main rainbelts covering the target regions in Figures 2a–2b rather than using the corresponding PCs, the correlation coefficients presented above would be higher. The qualitative conclusions, however, should remain the same. In addition, the latitude position of the largest correlation between the PC and the 200 hPa divergent fields is about 2.5 degrees north of the main rainbelt due to the frontal slope toward the cold air (figures omitted).

[22] *Sathiyamoorthy et al.* [2004] stated a significant association between the high-cloud amount and the speed

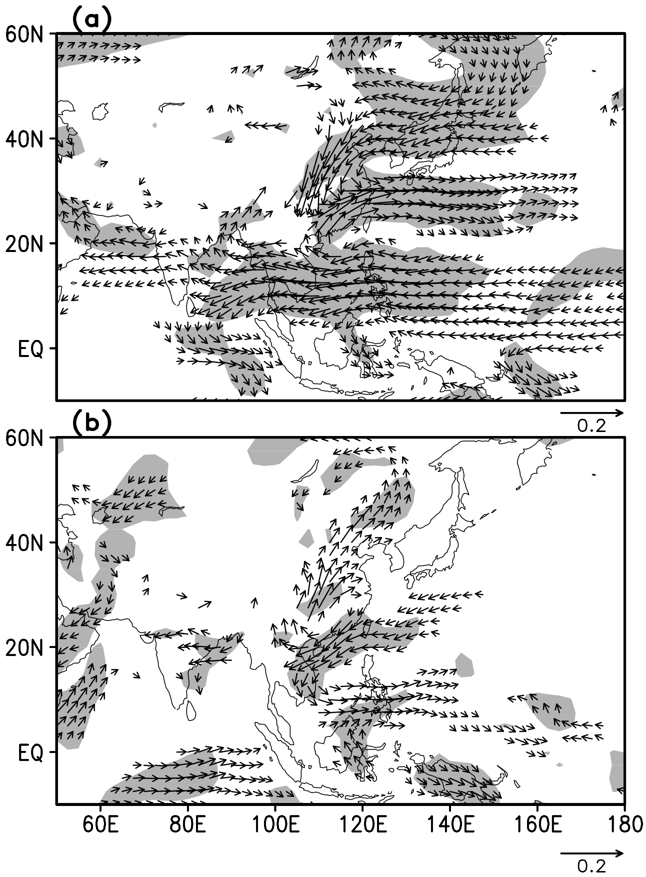

Figure 7. Regression of anomalous 850-hPa water vapor transport upon (a) PC1 and (b) PC2 of JJA rainfall EOF. Shaded regions are significant at the 95% confidence level. Units are kg $\times$ m^{-1} s^{-1}.

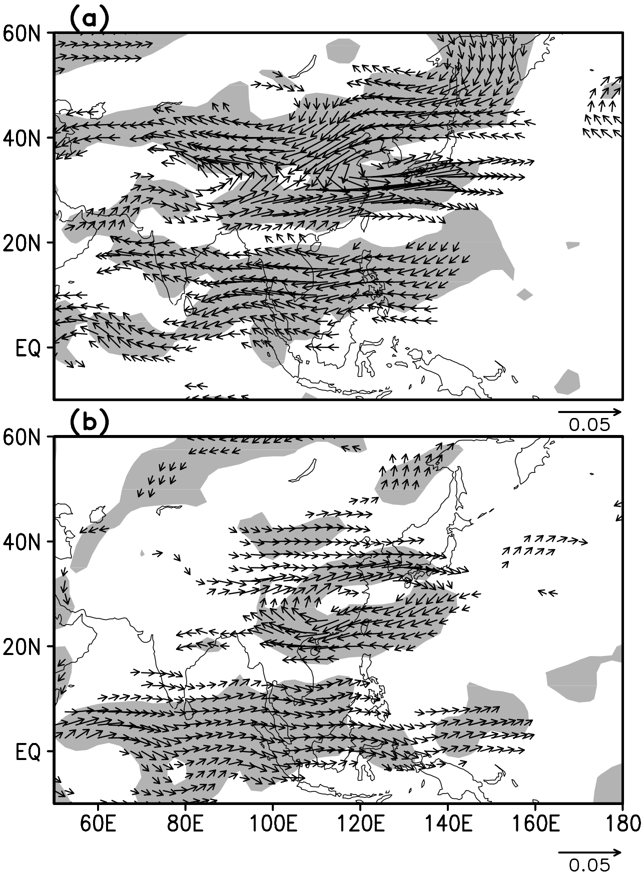

Figure 8. Same as Figure 7 except for the 500-hPa water vapor transport.

of the easterly jet over the South Asian monsoon region. The strong wind shear sweeps the cloud tops and may be unfavorable for cloud growth beyond about 300 hPa. Analyses presented above indicate that the significant association between the East Asian westerly jet stream and the monsoon rainfall results from the high level (200 hPa) divergent activity. *Yu et al.* [2004] found that the midtropospheric divergence coincides very well with the amount of nimbostratus and altostratus clouds throughout the year over southwest China. This finding partly supports the results presented here.

4.2. Vertical Distribution of Water Vapor Transport

[23] The existence of complex topography over the East Asia domain makes the estimation of the vertically integrated total moisture flux a difficult task. Although the surface pressure p_s is used to remove the impact of topography, i.e., the water vapor was set to zero at pressure levels below the p_s, and in light of the coarse vertical resolution of the reanalysis data, uncertainties related to the vertical integration in the above analyses should be estimated. For this purpose, the anomalous water vapor transport at each single standard pressure level is regressed upon the PCs of typical anomalous rainfall patterns. The results of 850 hPa and 500 hPa are shown in Figures 7 and 8, respectively. Generally speaking, the anomalous water vapor transport in the lower atmosphere closely resembles the pattern of the total transport shown in Figures 4a and 5a. This situation can clearly be seen in the anomaly patterns of 1000 hPa and 925 hPa (figures omitted) and 850 hPa (Figure 7). The cause can be attributed to the fact that the atmospheric moisture is concentrated mainly in the lower atmosphere and the situation of the vertically integrated water vapor transport is essentially dominated by the contribution of the lower atmosphere.

[24] Although as the common knowledge of climatology (seasonal mean), temperature is high over land and low over ocean in summer, examinations on the anomalous temperature field associated with the typical rainfall patterns demonstrate that the flow from the south is still warmer than that from the north in the context of anomaly field (figures omitted). Comparing Figure 7 with Figure 8 reveals that the northward transport of warm tropical water vapor occurs mainly in the lower atmosphere, while the transport of midlatitude cold water vapor occurs briefly in the upper atmosphere. This situation is much clearer in the Figures 7b and 8b. The typical feature of Figure 7b is the northward transport of lower latitude warmer water vapor. The eastward midlatitude water vapor transport is more obvious in Figure 8 than in Figure 7. Since the distribution of air moisture expressed as specific humidity steadily decreases from tropical lower latitudes northward to higher subtropical and midlatitudes (figure omitted), the main role of tropical water vapor transport is to provide abundant moisture, while the responsibility of colder midlatitude branches of water vapor transport is to block off the further northward penetration of the warmer moist flows originating from

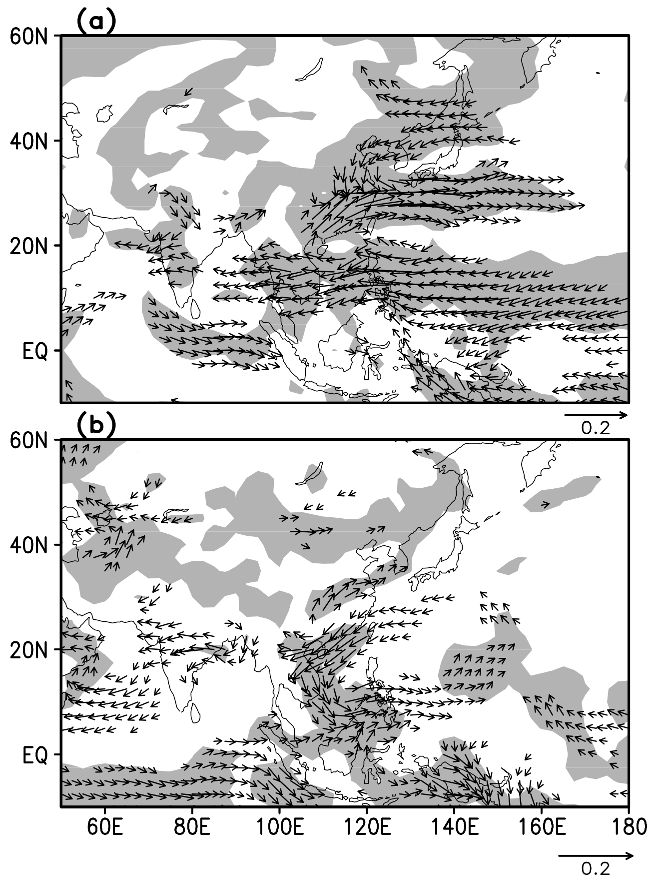

Figure 9. Same as Figure 7 except for ERA40 data.

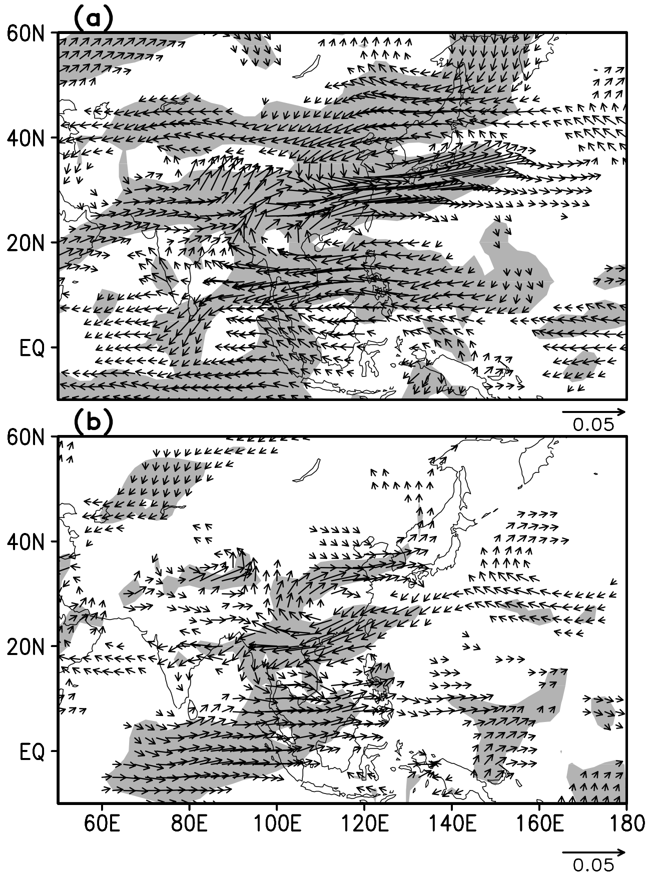

Figure 10. Same as Figure 8 except for ERA40 data.

lower latitudes. The conflict of the warm/wet air with the cold/dry air eventually results in the strong convergence over the main rainbelts, which provides a highly beneficial background of water vapor supply for the abundant anomalous rainfall.

[25] It should be stressed that the coincidence of the water vapor transport at single levels with that of the vertically integrated total transport in general patterns, particularly in origins of the main water vapor flows, demonstrates the credibility of the latter. The impact of topography does not disturb seriously the accurate estimation of the total water vapor transport in this analysis. As can be seen in Figure 1a, the strong summer monsoon rainfall variability occurs mainly east of 105°E where there is nearly no large or steep topography in comparison with the western plateau region. The ‘‘plain-like’’ topography of eastern China relative to western China gives the vertical integration an acceptable accuracy.

4.3. Water Vapor Transport Revealed by the ERA40 Data Set

[26] It is already known that the NCEP/NCAR reanalysis data have a problem in the East Asian area around the middle of the 1970s [*Yang et al.*, 2002]. In order to confirm the above findings regarding the water vapor transport, it is necessary to use other independent data to verify the results. The recently released ERA40 data provides an opportunity for such a comparison. The results given in Figures 7 and 8 are re-examined by using the ERA40 data (see Figures 9 and 10). Comparisons of the results using the two different data sets show consistent features of the anomalous water vapor transport over the target regions, e.g., the pathways and convergence of the tropical and subtropical water vapor along the middle and lower reaches of the Yangtze River valley associated with anomalous rainfall pattern 1, and the northward transport of the tropical water vapor along eastern China to the region between the lower reaches of the Yellow River valley and the Yangtze River valley associated with anomalous rainfall pattern 2 at 850 hPa.

[27] The intensities of water vapor transports in the ERA40 data are, however, generally weaker than those in the NCEP/NCAR data. Examples include the northward extension of the tropical water vapor transport along eastern China at 850 hPa. In the ERA40 data, the northward transports of the tropical water vapor are restricted to the lower reaches of the Huaihe River valley (Figure 9b). In the NCEP/NCAR data, the water vapor penetrates even more northward and further extends to the area north of the Korean Peninsula after crossing the Chinese Bohai Sea (Figure 7b). The situation for the difference between the two data sets at 500 hPa is slightly different. Compared with the conditions of 850 hPa, there is a closer similarity between these data sets in the general situation of the 500 hPa anomalous water vapor transport (see Figure 8 and Figure 10). These kinds of close similarity exist in the water vapor transports associated with the two typical anomalous rainfall patterns. This close agreement indicates a nearly negligible impact of the formerly noted NCEP/NCAR data problem on the water vapor transport estimation addressed here in view of a qualitative comparison. What we should stress here is that although the NCEP/NCAR data seem to provide a stronger water vapor transport in the low level atmosphere in comparison with that of the ERA40 data, generally these two data sets coincide well in the origins and transports of the water vapor transport associated with the typical anomalous summer rainfall patterns of China.

5. Concluding Remarks

[28] The vertically integrated atmospheric water vapor transports associated with typical anomalous summer rainfall patterns of China are analyzed by using the observational precipitation data and the NCEP/NCAR and ERA40 reanalysis data. The key results are summarized in Table 1.

[29] The main rainbelts associated with typical anomalous rainfall patterns of China are significantly correlated with the convergence of the water vapor transport and deep convections there. The origins of the water vapor supply related to these typical anomalous rainfall patterns are different than that related to the normal monsoon rainfall, and the tropical West Pacific plays an important role in supplying the water vapor. The pluvious middle and lower reaches of the Yangtze River valley are supported by water vapor coming directly from the Bay of Bengal and the South China Sea, but originally from the Philippine Sea. The heavier rainfall along the Huaihe River valley is favored by the subtropical southwest water vapor coming directly from the South China Sea. The origin of the water vapor is, however, ultimately the East China Sea and the adjacent subtropical Pacific further east along 20–25°N; but the Bay of Bengal contributes nothing.

[30] The anomalous water vapor transports are determined by the large-scale circulation changes. The position of the western Pacific subtropical high dominates the water vapor transports for the typical anomalous rainfall patterns, and the change of the East Asian jet stream favors the upper divergence related to deep convection. Wave propagation in East Asia resembling the PJ/EAP teleconnection pattern stands out in the circulation changes associated with the heavier rainfall along both the Yangtze River valley and the Huaihe River valley.

[31] The concentration of the water vapor in the lower atmosphere makes the anomalous total water vapor transport closely resemble that at the lower troposphere. The northward transport of warm water vapor occurs mainly in the lower atmosphere, while the transport of midlatitude cold water vapor occurs briefly in the upper atmosphere. The ERA40 data agree well with the NCEP/NCAR reanalysis data in the origins and transport of the water vapor associated with typical anomalous summer rainfall patterns of China, although they are weaker than the NCEP/NCAR data at the lower atmosphere in terms of quantitative comparison.

[32] **Acknowledgments.** This work was jointly supported by the National Natural Science Foundation of China under grants 40375029 and 40233031 and the "Knowledge Innovation Programs of the Chinese Academy of Sciences" under grant KZCX3-SW-221. The authors thank NCEP/NCAR and ECMWF for releasing reanalysis data. The insightful comments and helpful suggestions from two anonymous reviewers are highly appreciated.

References

Ding, Y. H. (1994), *Monsoons Over China*, 90 pp., Springer, New York.

Ding, Y. H., and G. Q. Hu (2003), A study on water vapor budget over China during the 1 998 severe flood periods, *Acta Meteorol. Sinica*, *61*(2), 129–145.

Ding, Y. H., and Y. Sun (2001), A study on anomalous activities of east Asian summer Monsoon during 1999, *J. Meteorol. Soc. Jpn.*, *79*, 1119–1137.

Gong, D., and C. Ho (2002), Shift in the summer rainfall over the Yangtze River valley in the late 1970s, *Geophys. Res. Lett.*, *29*(10), 1436, doi:10.1029/2001GL014523.

Gong, D., and C. Ho (2003), Arctic oscillation signals in the east Asian summer monsoon, *J. Geophys. Res.*, *108*(D2), 4066, doi:10.1029/2002JD002193.

Hu, Z.-Z. (1997), Interdecadal variability of summer climate over east Asia and its association with 500–hPa height and global sea surface temperature, *J. Geophys. Res.*, *102*, 19,403–19,412.

Hu, Z., S. Yang, and R. Wu (2003), Long-term climate variations in China and global warming signals, *J. Geophys. Res.*, *108*(D19), 4614, doi:10.1029/2003JD003651.

Huang, R. H., and F. Y. Sun (1992), Impacts of the tropical western Pacific on the east Asian summer monsoon, *J. Meteorol. Soc. Jpn.*, *70*, 243–256.

Huang, R. H., Z. Zhang, and G. Huang (1998), Characteristics of the water vapor transport in east Asian monsoon region and its difference from that in south Asian monsoon region in summer (in Chinese), *Sci. Atmos. Sinica*, *22*, 460–469.

Kalnay, E., et al. (1996), The NCEP/NCAR 40-year reanalysis project, *Bull. Am. Meteorol. Soc.*, *77*, 437–472.

Lau, K. M., and M. S. Li (1984), The monsoon of east Asia and its global associations—A survey, *Bull. Am. Meteorol. Soc.*, *65*, 114–125.

Li, C. F., and M. Yanai (1996), The onset and interannual variability of the Asian summer monsoon in relation to land-sea thermal contrast, *J. Clim.*, *9*, 358–375.

Meehl, G. A., and J. M. Arblaster (1998), The Asian-Australian monsoon and El Nino–Southern Oscillation in the NCAR climate system model, *J. Clim.*, *11*, 1356–1385.

Ninomiya, K. (1999), Moisture balance over China and the South China Sea during the summer monsoon in 1991 in relation to the intense rainfalls over China, *J. Meteorol. Soc. Jpn.*, *77*, 737–751.

Ninomiya, K., and C. Kobayashi (1999), Precipitation and moisture balance of the Asian summer monsoon in 1991 part II: Moisture transport and moisture balance, *J. Meteorol. Soc. Jpn.*, *77*, 77–99.

Nitta, T. (1987), Convective activities in the tropical western Pacific and their impact on the Northern Hemisphere summer circulation, *J. Meteorol. Soc. Jpn.*, *65*, 373–390.

Nitta, T., and Z.-Z. Hu (1996), Summer climate variability in China and its association with 500–hPa height and tropical convection, *J. Meteorol. Soc. Jpn.*, *74*, 425–445.

North, G. R., T. L. Bell, and R. F. Cahalan (1982), Sampling errors in the estimation of empirical orthogonal functions, *Mon. Weather Rev.*, *110*, 699–706.

Rasmusson, E. M., and K. C. Mo (1996), Large-scale atmospheric moisture cycling as evaluated from NMC global analysis and forecast products, *J. Clim.*, *9*, 3276–3297.

Ren, B. H., and R. H. Huang (1999), Interannual variability of the convective activities associated with the east Asian summer monsoon obtained from TBB variability, *Adv. Atmos. Sci.*, *16*, 77–90.

Sathiyamoorthy, V., P. K. Pal, and P. C. Joshi (2004), Influence of the upper-tropospheric wind shear upon cloud radiative forcing in the Asian monsoon region, *J. Clim.*, *17*, 2725–2735.

Simmonds, I., D. Bi, and P. Hope (1999), Atmospheric water vapor flux and its association with rainfall over China in summer, *J. Clim.*, *12*, 1353–1367.

Tao, S. Y., and L. X. Chen (1987), A review of recent research on the east Asian summer monsoon in China, in *Review of Monsoon Meteorology*, edited by C. P. Chang and T. N. Krishnamurti, pp. 60–92, Oxford Univ. Press, New York.

Trenberth, K. E., and C. J. Guiliemot (1995), Evaluation of the global atmospheric moisture budget as seen from analyses, *J. Clim.*, *8*, 2255–2272.

Wang, B., R. Wu, and X. Fu (2000), Pacific-east Asia teleconnection: How does ENSO affect east Asian climate?, *J. Clim.*, *13*, 1517–1536.

Wang, S. W., J. Cai, J. Zhu, and D. Gong (2002), The interdecadal variations of annual precipitation in China during 1880s–1990s (in Chinese), *Acta Meteorol. Sinica*, *60*, 637–639.

Wang, W. C., W. Gong, and H. L. Wei (2000), A regional model simulation of the 1991 severe precipitation event over the Yangtze-Huai River Valley: Part I: Precipitation and circulation statistics, *J. Clim.*, *13*, 74–92.

Webster, P. J. (1994), The role of hydrological processes in ocean-atmosphere interactions, *Rev. Geophys.*, *32*, 427–476.

Webster, P. J., and S. Yang (1992), Monsoon and ENSO: Selectively interactive systems, *Q. J. R. Meteorol. Soc.*, *118*, 160–173.

Xiao, H. P., and D. Y. Gong (2000), Comparison of the impact of ENSO on the rainfall over south China and India (in Chinese), *J. Natural Disasters*, *9*, 74–80.

Xie, Y. B., and W. J. Dai (1959), The calculation for some cases of the moisture transport over Yangtze River basin (in Chinese), *J. Appl. Meteorol. Sci.*, *13*, 67–77.

Xu, S. Y. (1958), China's water vapor transfer and budget (in Chinese), *Acta Meteorol. Sinistra*, *29*, 33–43.

Yang, S., K. M. Lau, and K. M. Kim (2002), Variations of the east Asian jet stream and Asian-Pacific-American winter climate anomalies, *J. Clim.*, *15*, 306–325.

Yu, R.-C., B. Wang, and T.-J. Zhou (2004), Climate effects of the deep continental stratus clouds generated by the Tibetan Plateau, *J. Clim.*, *17*, 2702–2713.

Zhai, P., and R. E. Eskridge (1997), Atmospheric water vapor over China, *J. Clim.*, *10*, 2643–2652.

Zhang, R. H. (2001), Relations of water vapor transport from Indian monsoon with that over east Asia and the summer rainfall in China, *Adv. Atmos. Sci.*, *18*, 1005–1017.

Zhao, Z.-G. Eds. (1999), *Summertime Floods and Droughts in China and the Associated Circulations* (in Chinese), 297 pp., Meteorol. Press, Beijing.

Zhou, T.-J. (2003), Comparison of the global air-sea freshwater exchange evaluated from independent data sets, *Prog. Natural Sci.*, *13*(8), 626–631.

Zhou, T.-J., and Z.-X. Li (2002), Simulation of the east Asian summer monsoon by using a variable resolution atmospheric GCM, *Clim. Dyn.*, *19*, 167–180.

Zhou, T.-J., X.-H. Zhang, and S.-W. Wang (1999), The air-sea freshwater exchange derived from NCEP/NCAR reanalysis data (in Chinese), *Acta Meteorol. Sinica*, *57*(3), 264–282.

R.-C. Yu and T.-J. Zhou, LASG, Institute of Atmospheric Physics, Chinese Academy of Sciences, Beijing 100029, China. (yrc@lasg.iap.ac.cn; zhoutj@lasg.iap.ac.cn)

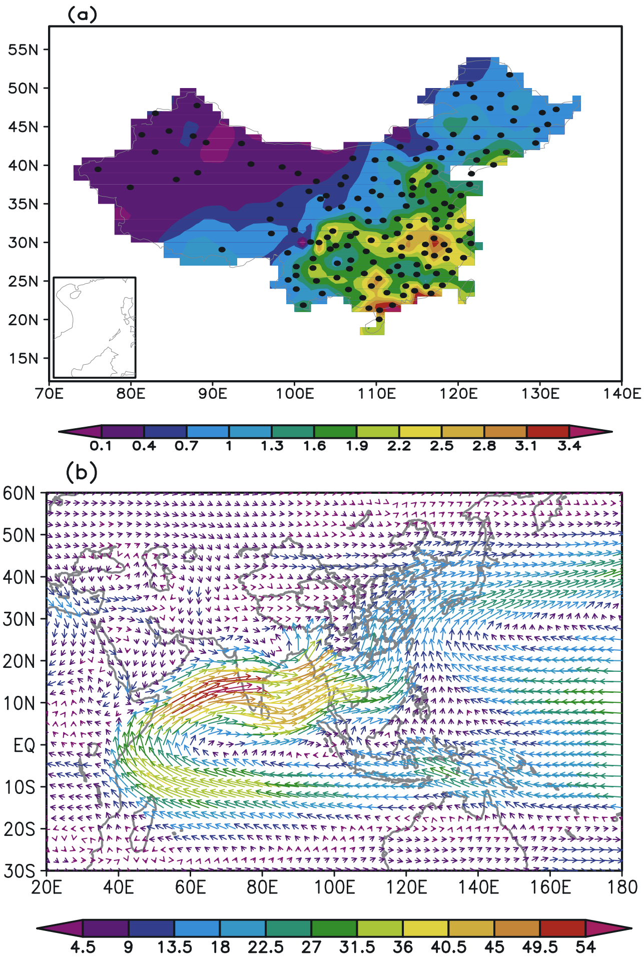

Figure 1. (a) Standard deviation of JJA mean rainfall revealed by the station data (mm/day). Dots indicate locations of the observational stations. (b) Vertically integrated climate mean (1951–1999 average) JJA water vapor transport (kg × m^{-1} s^{-1}). The coloring indicates the magnitude of the moisture flux vector.

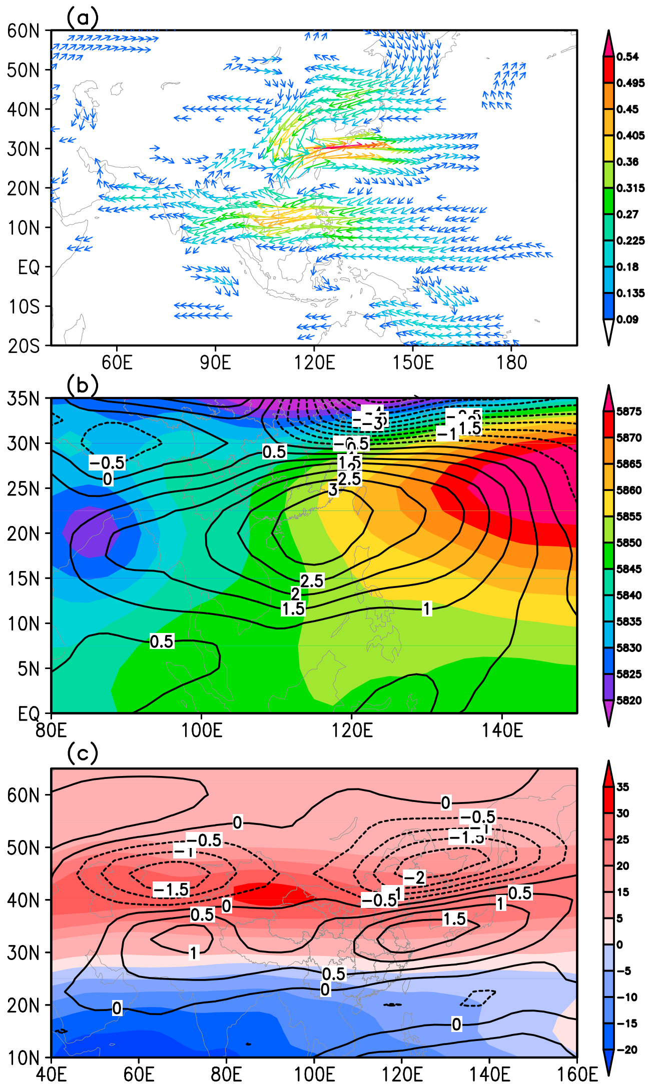

Figure 4. Anomalies of (a) vertically integrated water vapor transport in kg × $m^{-1}s^{-1}$, (b) 500–hPa geopotential height in meters, and (c) 200-hPa zonal wind in ms^{-1} regressed upon the PC of rainfall EOF1. The coloring in Figure 4a indicates the magnitude of the moisture flux vector. The climate mean conditions of Z500 and U200 are the colored backgrounds of Figures 4b and 4c, respectively.

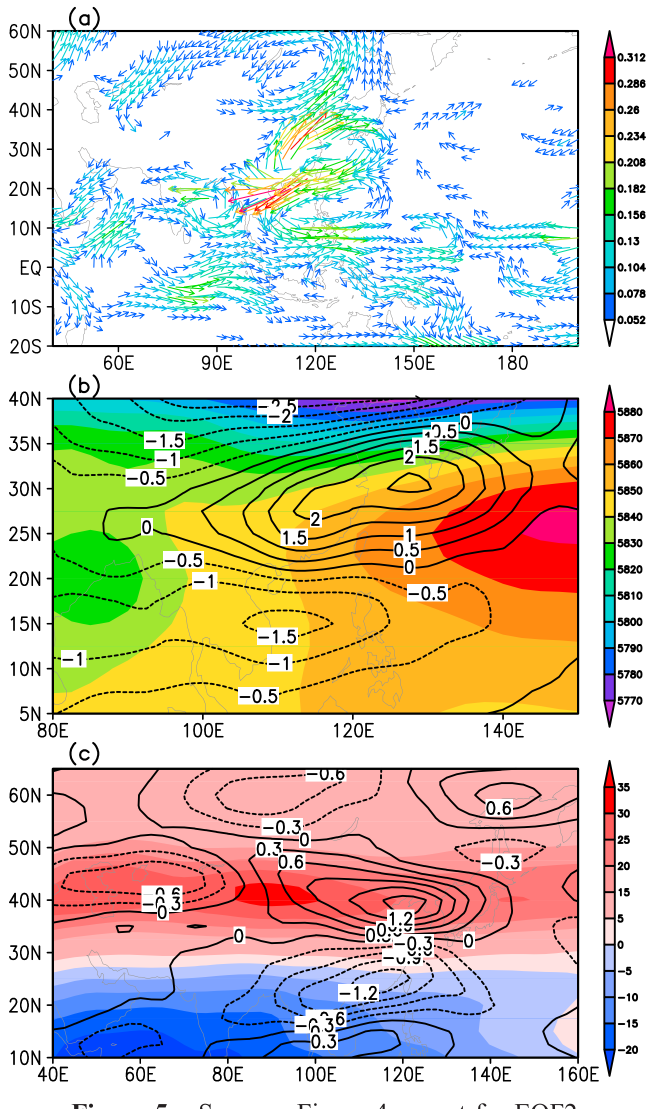

Figure 5. Same as Figure 4 except for EOF2.